



# Novel and Highly Efficient Conversion of Carbon Dioxide to Cyclic Carbonates Using Benzotriazolium Ionic Liquid-Modified Periodic Mesoporous Organosilica as a Heterogeneous and Recyclable Nanocatalyst

Xiao BingLiu<sup>1</sup> · Yu Lin Hu<sup>2</sup>

Received: 22 April 2020 / Accepted: 5 September 2020 / Published online: 17 September 2020  
© Springer Nature B.V. 2020

## Abstract

In the present study, we demonstrated the synthesis of copper oxychloride anionic benzotriazolium ionic liquid-modified periodic mesoporous organosilica PMO@ILCu<sub>2</sub>(OH)<sub>3</sub>Cl<sub>2</sub>(x) as efficient and green retrievable heterogeneous nanocatalysts for the synthesis of cyclic carbonates via cycloaddition of CO<sub>2</sub> with epoxides. Compared to other nanocatalysts, a superior catalytic activity was observed with PMO@ILCu<sub>2</sub>(OH)<sub>3</sub>Cl<sub>2</sub>(1.0), giving excellent yields and selectivities *under solvent-* and cocatalyst-free conditions. We also found that the existence of intensification synergistic effects from the hydroxyl groups sites of periodic mesoporous organosilica and the active sites of the functionalized ionic liquid, resulting in the enhanced catalytic *activity*. The catalytic process displayed ease of recovery, excellent stability and recyclability for at least five runs without significant loss of its catalytic activity. The developed catalytic system is proven to be a powerful tool for the chemical fixation of CO<sub>2</sub> with epoxides to produce the cyclic carbonates.

**Keywords** Immobilized ionic liquid · Periodic mesoporous organosilica · Synergistic catalysis · Cycloaddition · Cyclic carbonates

## 1 Introduction

Chemical fixation of carbon dioxide (CO<sub>2</sub>) into value-added chemicals has attracted widespread attention recently, as CO<sub>2</sub> is an abundant, inexpensive, nontoxic C1 source as well as being the primary greenhouse gas [1–6]. Among possible processes, the transformation of CO<sub>2</sub> with epoxides into cyclic carbonates has 100% atom efficiency and is one of the most valuable and sustainable strategies. Cyclic carbonates have been widely used as raw materials in pharmaceuticals, fuel additives, electrolytes and fine chemicals [7–9]. Therefore, there has been a growing interest in the synthesis of cyclic carbonates, and a number of catalytic systems have been developed for the synthesis of cyclic carbonates, including metal

complexes [10–12], organocatalysts [13, 14], Lignin/KI [15], B<sub>2</sub>O<sub>3</sub>/*n*Bu<sub>4</sub>NBr [16], MOFs [17–19], NH<sub>3</sub>I-Zn/SBA-15 [20], WP-KI [21], Cu<sub>6</sub> cluster/*n*Bu<sub>4</sub>NBr [22], CoPc/TiO<sub>2</sub> [23], and others [24–26]. However, most of these catalyst systems suffer from drawbacks associated with the use of expensive reagents, harsh reaction conditions, relatively rare availability and catalyst reusability problems. Therefore, the development of catalytic systems that are both efficient and environmentally benign for the synthesis of cyclic carbonates still poses a considerable challenge.

Ionic liquids (ILs) have been of much interest as they have a wide range of applications in the areas of separation, catalysis and industrial chemistry [27–30]. Especially, metal-containing ionic liquids have been successfully used as catalysts in catalytic synthesis, which combine the advantages of both ionic liquid and transition metal catalysis and often leading to improved catalytic performance comparing to the classical ionic liquids [31, 32]. In this respect, many ILs including metal-containing ILs have been synthesized and they exhibited good catalytic performance in the transformation of CO<sub>2</sub> into cyclic carbonates [33–37]. Despite these advances, these catalytic systems often suffer from some disadvantages such

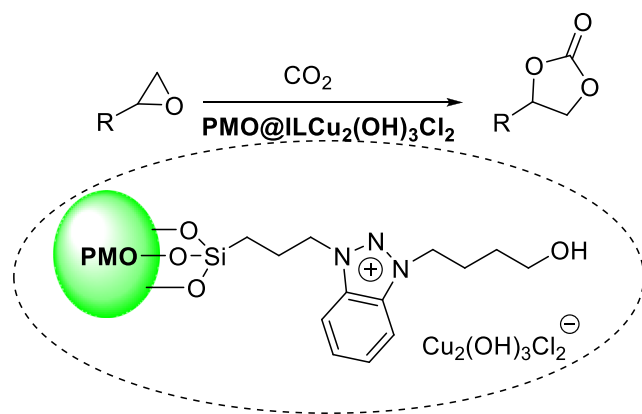
✉ Yu Lin Hu  
huyulin1982@163.com

<sup>1</sup> College of Chemistry and Chemical Engineering, Jinggangshan University, Ji'an 343009, People's Republic of China

<sup>2</sup> College of Materials and Chemical Engineering, China Three Gorges University, Yichang 443002, People's Republic of China

as ILs separation and recyclability. To facilitate easy separation and recycling of catalyst, heterogeneous catalysis offer an alternative strategy for improving recyclability [38–47]. Thus, the development of highly efficient and easily recyclable heterogeneous catalysts in combination with the characteristics of homogeneous ILs is highly desirable. The immobilization of ionic liquids on silica supports materials have been explored as develop novel and promising heterogeneous supported ionic liquids [48–53], which is a versatile way to keep ionic liquid and support tightly together and *simplify* separation, improve their catalytic activity and *reusability*. Among silica-based materials, periodic mesoporous organosilicas (PMOs) have attracted significant research interests because of their uniform and tunable pore sizes, highly ordered mesostructure, large surface areas and heterogeneous functional moieties distribution properties [54–57]. Especially, the introduction of active sites into PMOs for the synthesis of functionalized PMOs towards specific application demands in the fields of separation and catalysis has attracted a lot of attention [58–64]. Likewise, the immobilization of functionalized ILs on periodic mesoporous organosilicas and led to the formation of ionic liquid-functionalized PMOs, which were expected to afford highly useful catalytic materials retaining properties of the both moieties.

In the light of these considerations, the present work would to introduce the immobilization of novel benzotriazolium ionic liquid onto periodic mesoporous organosilica to fabricate multifunctional ionic liquid-based PMOs nanomaterials. These resulting new modified mesoporous nanomaterials with different *loading* levels of IL have been evaluated as recoverable catalysts for chemical fixation of CO<sub>2</sub> with epoxides in the absence of nucleophilic cocatalyst and solvent (Scheme 1). We were delighted to find that these as-synthesized nanocatalysts exhibit an enhancement in the catalytic activity for conversion of CO<sub>2</sub> to cyclic carbonates, by which high yields and selectivities could be obtained under relatively moderate conditions. Additionally, we also found that the nanocatalyst acts as an excellent synergic catalyst in which



**Scheme 1** Chemical fixation of CO<sub>2</sub> with epoxides catalyzed by PMO@ILCu<sub>2</sub>(OH)<sub>3</sub>Cl<sub>2</sub>

the catalytic activity could be boosted by the immobilized functional groups of IL and hydroxyl active sites on the PMO framework. The proposed multifunctional nanocatalyst is found to be highly effective for the homogeneous catalytic cycloaddition and easily heterogeneous reusable for several consecutive cycles, which offers a new solution for green and recyclable catalytic synthesis of cyclic carbonates with high performance and sustainable efficiency.

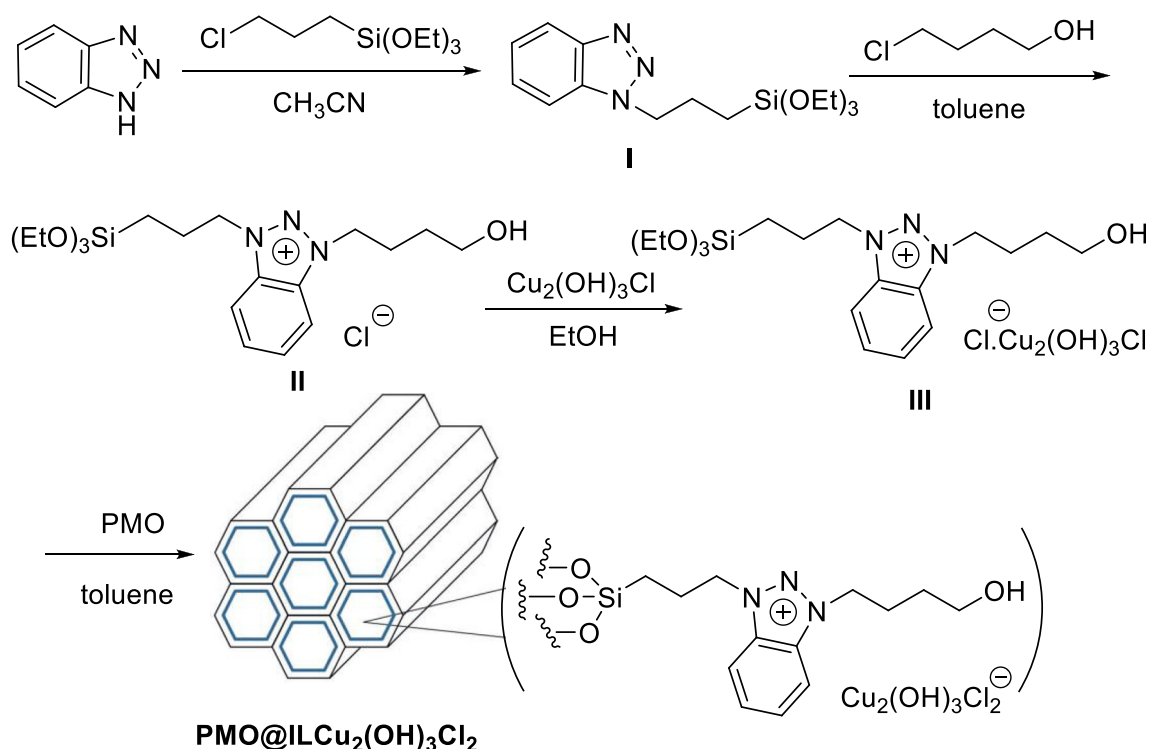
## 2 Experimental

### 2.1 General

All reagents are analytical grade and used without further purification. Pluronic 123 (EO<sub>20</sub>PO<sub>70</sub>EO<sub>20</sub>) and 1,2-bis(triethoxysilyl)ethane were obtained from Sigma-Aldrich. The crystallinity of the samples was analyzed by powder X-ray diffraction (XRD) using a Ultima IV diffractometer with Cu K<sub>α</sub> radiation (λ = 0.15406 nm) radiation. Fourier transform infrared (FT-IR) spectra were recorded on a Nicolet 6700 spectrometer in the range of 400–4000 cm<sup>-1</sup> using KBr pellets. The morphology of the samples was investigated by using scanning electron microscopy (SEM, JSM-7500F) with operating voltage at 10 kV equipped with energy dispersive spectroscopy (EDS). UV-Vis spectra were recorded using a Shimadzu UV-2450 spectrophotometer with an integrating sphere attachment within the range of 200 to 800 nm and with BaSO<sub>4</sub> as the reflectance standard. The thermogravimetric analysis (TGA) experiments were performed on a NETZSCH STA 449 F5 apparatus in the range of 30–600 °C with heating rate of 10 °C/min. The BET surface areas and pore volumes of samples were calculated using the BET method from nitrogen adsorption-desorption, using a BELSORP-max apparatus measured at liquid nitrogen temperature (77 K). The samples were degassed under vacuum at 120 °C for 6 h before measurements. Gas chromatography analysis were performed on a Thermo Scientific TRACE1300 analyzers assembled with TG-OCP 30 m × 0.25 mm × 0.25 μm (Thermo Fisher) column and a flame ionization detector. <sup>1</sup>H NMR spectra were recorded on a Bruker 400 MHz spectrometer at room temperature and TMS as internal standard in CDCl<sub>3</sub>. Elemental analysis were obtained with an Carlo-Erba 1106 elemental analyzer.

### 2.2 Preparation of PMO@ILCu<sub>2</sub>(OH)<sub>3</sub>Cl<sub>2</sub>(x)

The general route for the preparation of nanomaterials PMO@ILCu<sub>2</sub>(OH)<sub>3</sub>Cl<sub>2</sub>(x) is shown in Scheme 2. PMO support was prepared according to literature method [55, 56]. The supported catalysts PMO@ILCu<sub>2</sub>(OH)<sub>3</sub>Cl<sub>2</sub> were prepared following similar procedures in literatures [27, 59, 60, 64]. Typically, (3-chloropropyl) triethoxysilane (0.2 mol) and



**Scheme 2** Schematic illustration of synthesis process for PMO@ILCu<sub>2</sub>(OH)<sub>3</sub>Cl<sub>2</sub>

1,2,3-benzotriazole (0.2 mol) were dispersed in acetonitrile (260 mL), and continuously stirred for 24 h at 80 °C. After the reaction, the solvent was removed by vacuum, and the crude product was washed with ethanol and dried at 60 °C for 4 h to give **I**. Then, **I** (0.1 mol) and 4-chloro-1-butanol (0.1 mol) were dissolved with 150 mL toluene in 250 mL round flask. The mixture was stirred for 24 h at 100 °C. After cooling to room temperature, the precipitate was isolated and washed with dichloromethane to give ILCI **II**. Afterwards, **II** (0.05 mol), copper oxychloride (0.05 mol), and ethanol (120 mL) were stirred at 60 °C for 48 h. The crude material was washed with ethanol-water and dried at 60 °C to give copper oxychloride anion-functionalized ionic liquid ILCu<sub>2</sub>(OH)<sub>3</sub>Cl<sub>2</sub> **III**. Finally, the immobilized ionic liquids with different mass ratio of ionic liquid to PMO were prepared. In a typical synthesis, PMO (1.0 g), **III** (x g) and toluene (100 mL) were refluxed for 24 h under nitrogen. After cooling to room temperature, the solid product was recovered by filtration and washed with acetone for removal the excess ionic liquid. Then the samples were dried under vacuum to give the supported nanocatalysts PMO@ILCu<sub>2</sub>(OH)<sub>3</sub>Cl<sub>2</sub>(x).

### 2.3 Catalytic Cycloaddition of Epoxides and CO<sub>2</sub>

Epoxide (0.1 mol), PMO@ILCu<sub>2</sub>(OH)<sub>3</sub>Cl<sub>2</sub>(1.0) (0.2 g) were added into a stainless-steel autoclave and then was purged with CO<sub>2</sub> for three times. The reactor was pressurized with CO<sub>2</sub> to 1.5 MPa and then heated to the desired temperature,

the mixture was maintained for a desired time under vigorous stirring. After completion of the reaction, the excess CO<sub>2</sub> was vented slowly. The catalyst was easily separated from the mixture by centrifugation, and the product were injected in a gas chromatography (Agilent 7890) equipped with FID detector for a quantitative analysis. The recovered catalyst was recycled directly for the next run. All of the products were identified by comparing their physical and GC data with those of the standard compounds.

### 2.4 Spectroscopic Data for the Products

Propylene carbonate (Table 2, entry 1): <sup>1</sup>H NMR (400 MHz, CDCl<sub>3</sub>, δ ppm) 1.45 (dd, CH<sub>3</sub>, 3H), 3.96 (t, CH, 1H), 4.54 (t, CH, 1H), 4.82–4.86 (m, CH, 1H); Elemental analysis for C<sub>4</sub>H<sub>6</sub>O<sub>3</sub>: C 47.06, O 47.01. Found C 47.01, O 46.98.

1,2-Butylene glycol carbonate (Table 2, entry 2): <sup>1</sup>H NMR (400 MHz, CDCl<sub>3</sub>, δ ppm) 0.97 (t, CH<sub>3</sub>, 3H), 1.58–1.60 (m, CH<sub>2</sub>, 2H), 4.43 (d, 2H); 4.59–4.63 (m, CH, 1H); Elemental analysis for C<sub>5</sub>H<sub>8</sub>O<sub>3</sub>: C 51.72, O 41.34. Found C 51.67, O 41.29.

1,2-Butylene glycol carbonate (Table 2, entry 3): <sup>1</sup>H NMR (400 MHz, CDCl<sub>3</sub>, δ ppm) 0.93 (t, CH<sub>3</sub>, 3H), 1.56–1.62 (m, CH<sub>2</sub>, 2H), 4.43 (d, 2H); 4.58–4.62 (m, CH, 1H); Elemental analysis for C<sub>4</sub>H<sub>6</sub>O<sub>4</sub>: C 40.68, O 54.19. Found C 40.62, O 54.15.

(Chloromethyl)ethylene carbonate (Table 2, entry 4): <sup>1</sup>H NMR (400 MHz, CDCl<sub>3</sub>, δ ppm) 3.76 (dd, CH<sub>2</sub>, 2H), 4.36

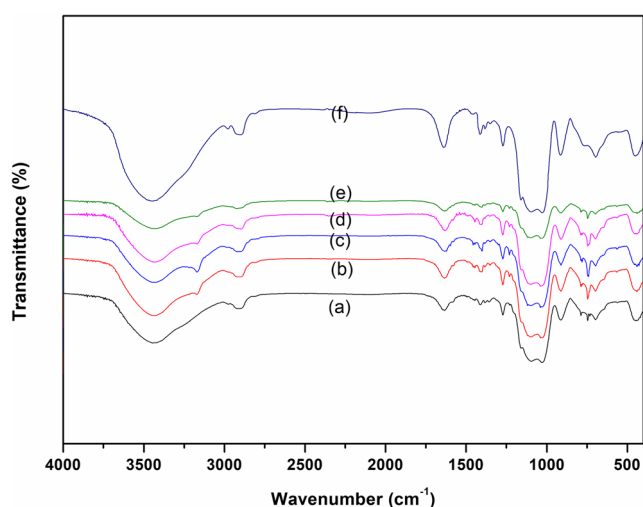
(t, CH<sub>2</sub>, 1H), 4.58 (t, CH<sub>2</sub>, 1H), 4.91–4.95 (m, CH, 1H); Elemental analysis for C<sub>4</sub>H<sub>5</sub>ClO<sub>3</sub>: C 35.19, Cl 25.96, O 35.15. Found C 35.15, Cl 25.93, O 35.08.

Hexahydrobenzo[d][1,3]dioxol-2-one (Table 2, entry 5): <sup>1</sup>H NMR (400 MHz, CDCl<sub>3</sub>, δ ppm) 1.34–1.48 (m, CH<sub>2</sub>CH<sub>2</sub>, 4H), 1.75–1.84 (m, 2CH<sub>2</sub>, 4H), 5.22 (t, 2CH, 2H); Elemental analysis for C<sub>7</sub>H<sub>10</sub>O<sub>3</sub>: C 59.15, O 33.76. Found C 59.09, O 33.73.

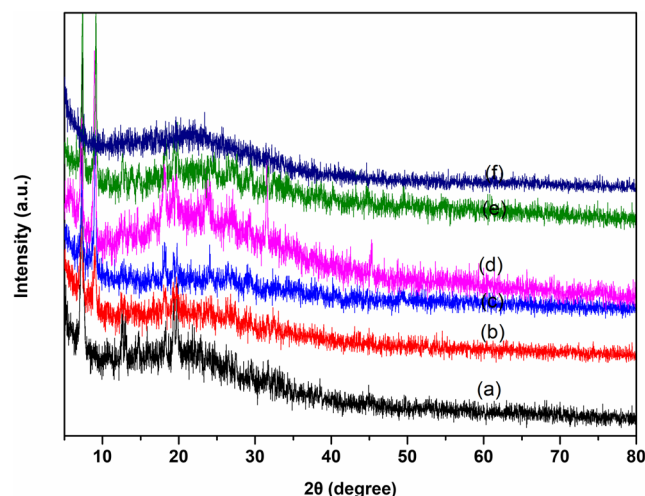
Styrene carbonate (Table 2, entry 6): <sup>1</sup>H NMR (400 MHz, CDCl<sub>3</sub>, δ ppm) 4.35 (t, CH<sub>2</sub>, 1H), 4.72 (t, CH<sub>2</sub>, 1H), 5.68 (t, CH<sub>2</sub>, 1H), 7.28–7.40 (m, Ar-H, 5H); Elemental analysis for C<sub>9</sub>H<sub>8</sub>O<sub>3</sub>: C 65.85, O 29.24. Found C 65.80, O 29.17.

### 3 Results and Discussion

The as-fabricated nanomaterials PMO@ILCu<sub>2</sub>(OH)<sub>3</sub>Cl<sub>2</sub>(x) were characterized by FT-IR analysis (Fig. 1). The adsorption peaks at around 1085 cm<sup>-1</sup>, 810 cm<sup>-1</sup>, and 486 cm<sup>-1</sup>, were assigned to the stretching vibration of Si–O. The characteristic bands at about 3518 cm<sup>-1</sup>, 1635 cm<sup>-1</sup> were attributed to the hydrogen-bonded stretching and bending vibrations [48–50], and the two peaks became weaker when the ionic liquid loading levels on PMO were increased. The peaks at about 1174 cm<sup>-1</sup>, and 1028 cm<sup>-1</sup> were attributed to N=N, and C–N stretching vibrations of triazolium ring. The characteristic bands around the range 1455–1610 cm<sup>-1</sup> and 3085 cm<sup>-1</sup>, were assigned to the stretching vibrations of aromatic ring [27, 65]. The characteristic bands around 2861 cm<sup>-1</sup>, 1298 cm<sup>-1</sup>, and 737 cm<sup>-1</sup> were attributed to the stretching vibrations of CH<sub>2</sub>. The characteristic bands that at around 729 cm<sup>-1</sup>, 1605 cm<sup>-1</sup> and 910 cm<sup>-1</sup> were ascribed to the C–Cl, Cu–Cl, Cu–O vibrational modes, respectively [66]. If the



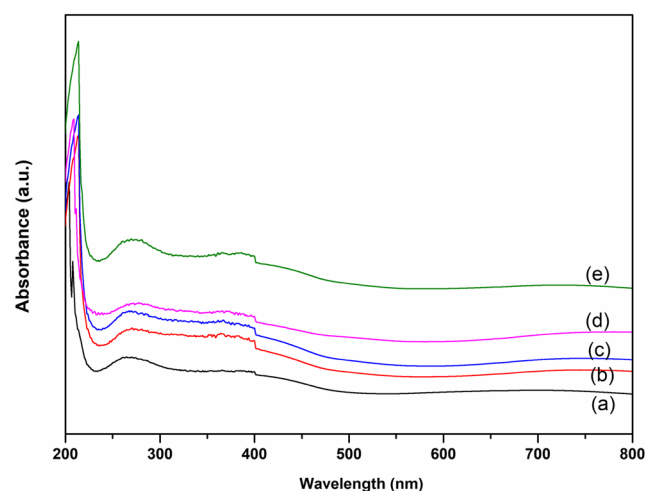
**Fig. 1** FT-IR spectras of PMO@ILCu<sub>2</sub>(OH)<sub>3</sub>Cl<sub>2</sub>(0.4) (a), PMO@ILCu<sub>2</sub>(OH)<sub>3</sub>Cl<sub>2</sub>(0.6) (b), PMO@ILCu<sub>2</sub>(OH)<sub>3</sub>Cl<sub>2</sub>(0.8) (c), PMO@ILCu<sub>2</sub>(OH)<sub>3</sub>Cl<sub>2</sub>(1.0) (d), PMO@ILCu<sub>2</sub>(OH)<sub>3</sub>Cl<sub>2</sub>(1.2) (e), and PMO (f)



**Fig. 2** XRD patterns of PMO@ILCu<sub>2</sub>(OH)<sub>3</sub>Cl<sub>2</sub>(0.4) (a), PMO@ILCu<sub>2</sub>(OH)<sub>3</sub>Cl<sub>2</sub>(0.6) (b), PMO@ILCu<sub>2</sub>(OH)<sub>3</sub>Cl<sub>2</sub>(0.8) (c), PMO@ILCu<sub>2</sub>(OH)<sub>3</sub>Cl<sub>2</sub>(1.0) (d), PMO@ILCu<sub>2</sub>(OH)<sub>3</sub>Cl<sub>2</sub>(1.2) (e), and PMO (f)

loading levels of ionic liquids were increased, it can be found that the two peaks at about 1174 cm<sup>-1</sup>, 729 cm<sup>-1</sup> became stronger and visible. The results indicated that the successful immobilization of functionalized benzotriazolium ionic liquid onto the PMO.

The XRD diffraction patterns for the nanomaterials PMO@ILCu<sub>2</sub>(OH)<sub>3</sub>Cl<sub>2</sub>(x) are shown in Fig. 2. The diffraction peak about 2θ = 22.5° is the characteristic diffraction peak of PMO [54, 55, 57–60]. Other diffraction peaks at about 2θ = 5.2°, 14.8°, 20.2°, and 32.4° compared to the parent PMO were belong to the crystal planes of copper anion of ionic liquid [67, 68]. No other peaks corresponding to ionic liquid were observed, suggested that the ionic liquid sites were well-dispersed on the PMO framework. These results



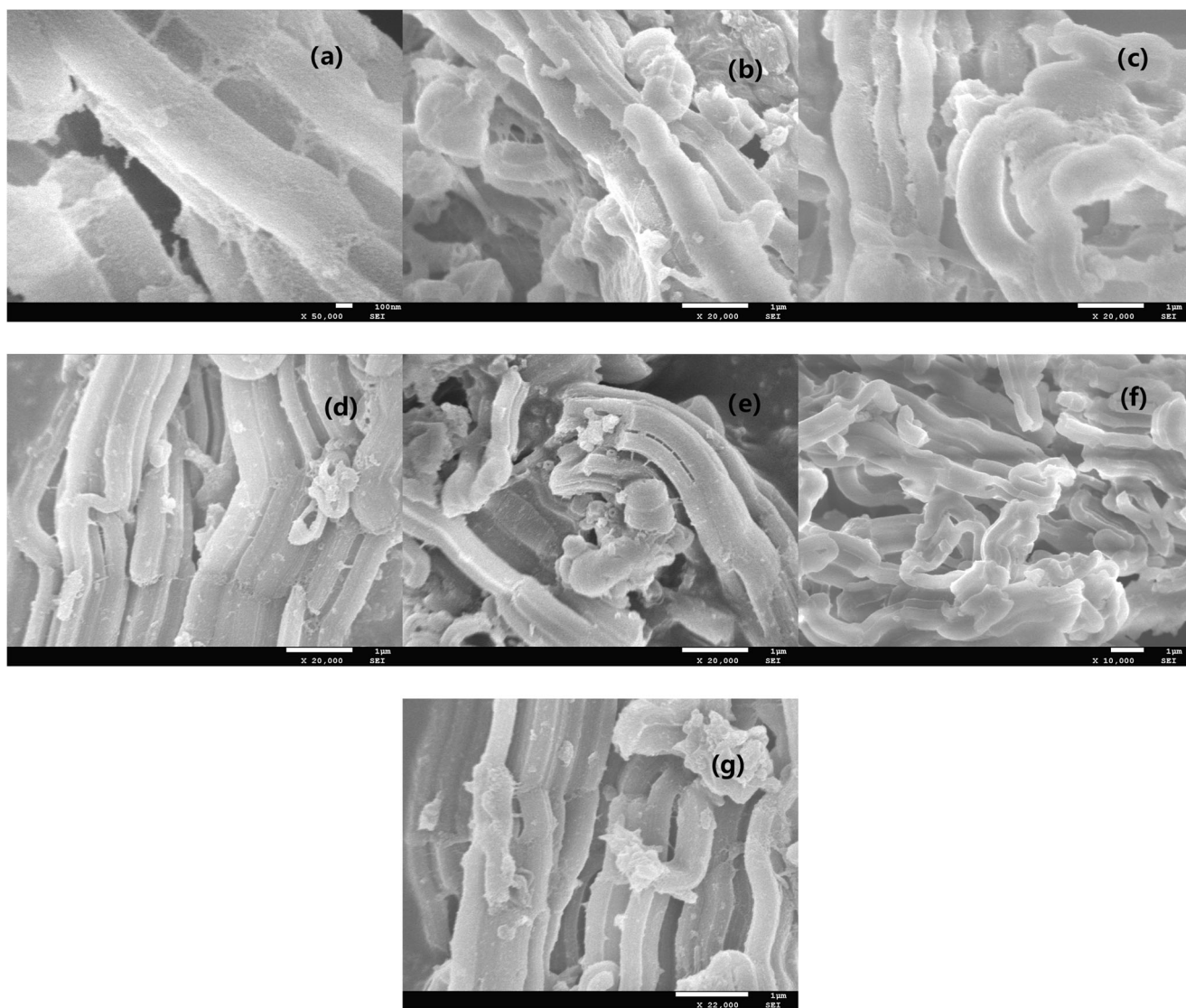
**Fig. 3** UV-Vis spectras of PMO@ILCu<sub>2</sub>(OH)<sub>3</sub>Cl<sub>2</sub>(0.4) (a), PMO@ILCu<sub>2</sub>(OH)<sub>3</sub>Cl<sub>2</sub>(0.6) (b), PMO@ILCu<sub>2</sub>(OH)<sub>3</sub>Cl<sub>2</sub>(0.8) (c), PMO@ILCu<sub>2</sub>(OH)<sub>3</sub>Cl<sub>2</sub>(1.0) (d), and PMO@ILCu<sub>2</sub>(OH)<sub>3</sub>Cl<sub>2</sub>(1.2) (e)

indicated that the basic crystalline structure of PMO framework maintained even after being immobilized of ionic liquid. Figure 3 shows UV–Vis spectra of the nanomaterials  $\text{PMO@ILCu}_2(\text{OH})_3\text{Cl}_2(x)$ . The main absorption band at around 232 nm, corresponding to the characteristic Si–O bands absorption of PMO [54, 58–61]. It can be seen from Fig. 3a–e that, the absence of peaks of immobilized ionic liquids in these nanomaterials confirmed that the ionic liquids species were uniform and homogeneous dispersed on the support framework.

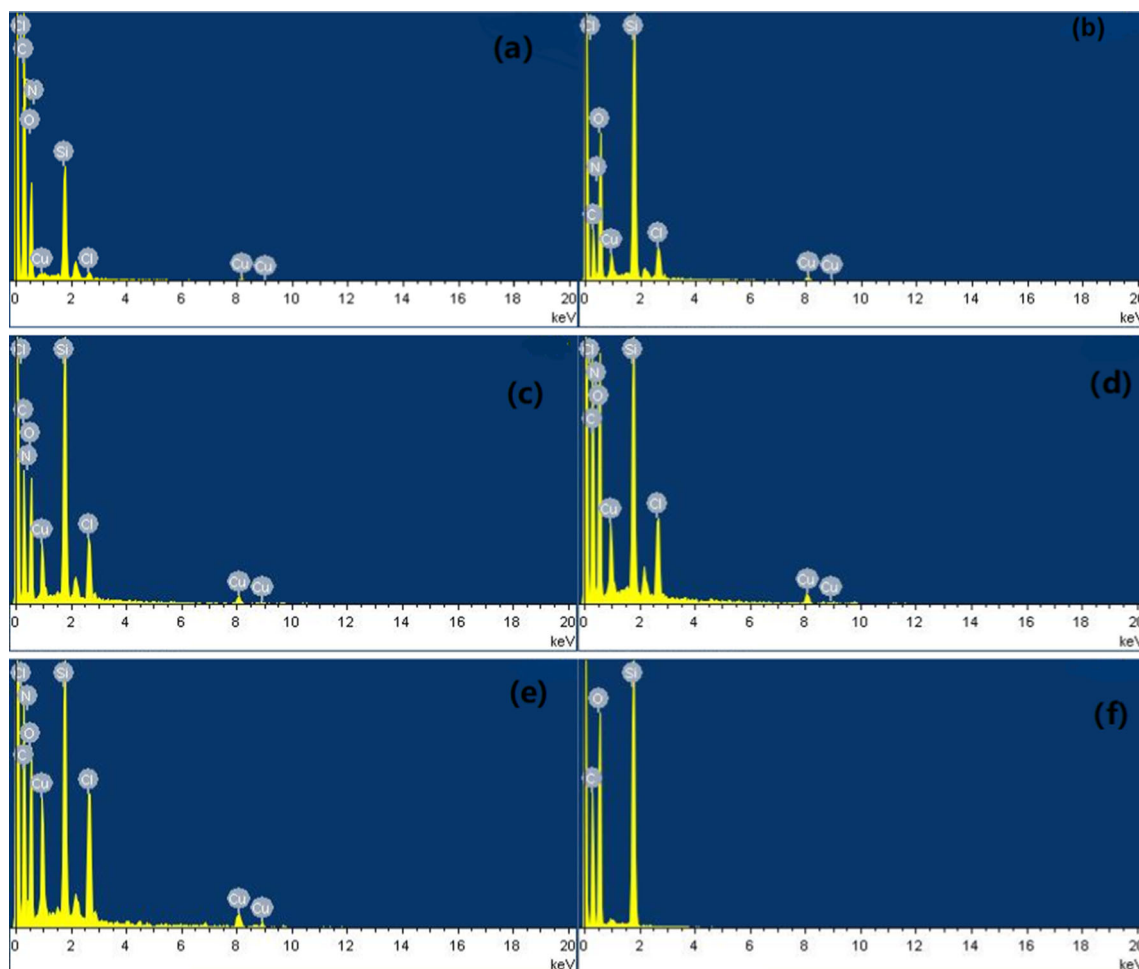
The SEM morphology of the synthesized nanomaterials is shown in Fig. 4. Figure 4f showed the characteristic morphological features of PMO [54–56]. Figures 4a–e SEM images of  $\text{PMO@ILCu}_2(\text{OH})_3\text{Cl}_2(x)$  demonstrated the rope-like morphology of aggregated small spherical particles. It can be seen

that both PMO and  $\text{PMO@ILCu}_2(\text{OH})_3\text{Cl}_2(x)$  exhibited similar and uniform rope-like morphology, indicating that the functional ionic liquid is attached to the inner tube wall of PMO and the immobilization of ionic liquid *do* not nearly change the surface morphology of PMO. Additionally, a more detailed investigation on the elemental composition of the nanocatalyst  $\text{PMO@ILCu}_2(\text{OH})_3\text{Cl}_2(1.0)$  was investigated by EDS (Fig. 5). The EDS analysis suggested that there existed the expected elemental signals of C, O, N, Cl, Cu and Si in the synthesized nanocomposites  $\text{PMO@ILCu}_2(\text{OH})_3\text{Cl}_2(x)$ .

The nitrogen adsorption-desorption isotherms and pore size distributions of the pure periodic mesoporous organosilica and  $\text{PMO@ILCu}_2(\text{OH})_3\text{Cl}_2(1.0)$  were determined (Fig. 6). Similar to the mesoporous structure of the pure PMO, the nanocatalyst exhibited the type IV isotherms with

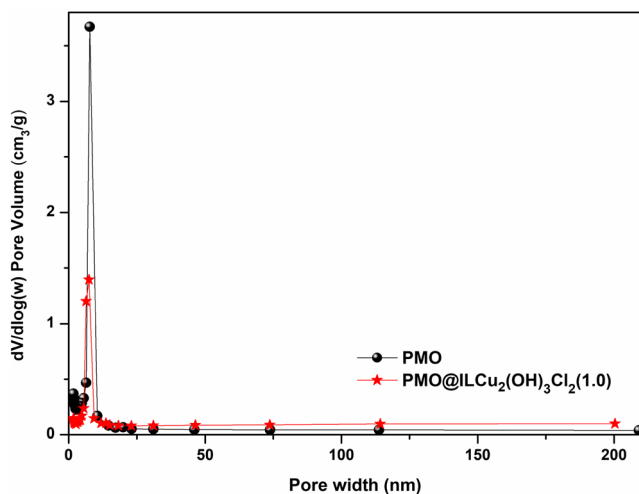


**Fig. 4** SEM images of  $\text{PMO@ILCu}_2(\text{OH})_3\text{Cl}_2(0.4)$  (a),  $\text{PMO@ILCu}_2(\text{OH})_3\text{Cl}_2(0.6)$  (b),  $\text{PMO@ILCu}_2(\text{OH})_3\text{Cl}_2(0.8)$  (c),  $\text{PMO@ILCu}_2(\text{OH})_3\text{Cl}_2(1.0)$  (d), and  $\text{PMO@ILCu}_2(\text{OH})_3\text{Cl}_2(1.2)$  (e), PMO (f), and five times recovered  $\text{PMO@ILCu}_2(\text{OH})_3\text{Cl}_2(1.0)$  (g)



**Fig. 5** EDS image of MO@ILCu<sub>2</sub>(OH)<sub>3</sub>Cl<sub>2</sub>(0.4) (a), PMO@ILCu<sub>2</sub>(OH)<sub>3</sub>Cl<sub>2</sub>(0.6) (b), PMO@ILCu<sub>2</sub>(OH)<sub>3</sub>Cl<sub>2</sub>(0.8) (c), PMO@ILCu<sub>2</sub>(OH)<sub>3</sub>Cl<sub>2</sub>(1.0) (d), PMO@ILCu<sub>2</sub>(OH)<sub>3</sub>Cl<sub>2</sub>(1.2) (e), and PMO (f)

hysteresis loops of subclass H4 [55–58]. The grafting of the ionic liquid on the organosilica carrier greatly influenced its surface area and pore volume, as well as slightly smaller pore

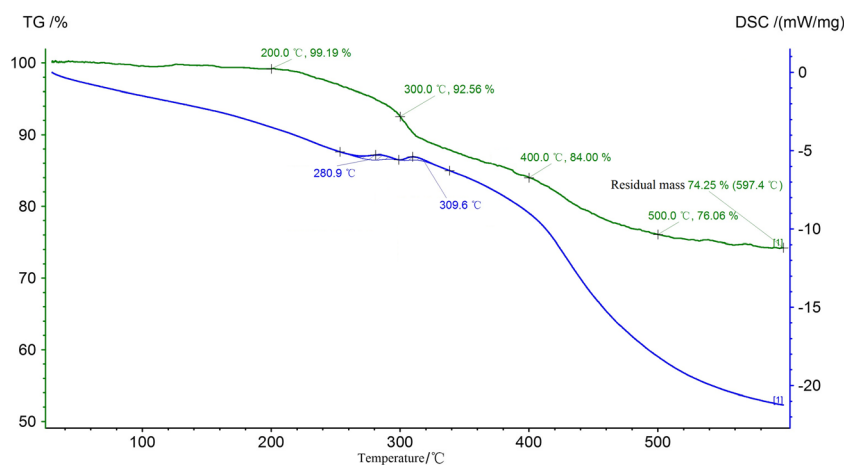


**Fig. 6** N<sub>2</sub> adsorption-desorption isotherms and pore size distributions of PMO@ILCu<sub>2</sub>(OH)<sub>3</sub>Cl<sub>2</sub>(1.0)

size. The results showed that the surface area, pore volume, pore size and were reduced from 571.59 m<sup>2</sup> g<sup>-1</sup>, 0.76 cm<sup>3</sup> g<sup>-1</sup> and 5.89 nm for PMO to 259.50 m<sup>2</sup> g<sup>-1</sup>, 0.43 cm<sup>3</sup> g<sup>-1</sup> and 5.54 nm for PMO@ILCu<sub>2</sub>(OH)<sub>3</sub>Cl<sub>2</sub>(1.0), respectively, which was due to the immobilization of ionic liquid on the organosilica carrier. The thermal stability of PMO@ILCu<sub>2</sub>(OH)<sub>3</sub>Cl<sub>2</sub>(1.0) was determined by thermal gravimetric analysis (TGA). The nanocatalyst depict a two main step thermal decomposition (Fig. 7). The first step of weight loss (0.81%) below 200 °C related to the removal of adsorbed water (≤100 °C) and other volatile *solvent residues* (100 ~ 200 °C), whereas the main weight loss (24.94%) from 200 to 600 °C in the second and third steps was corresponded to degradation of the organic moieties of ionic liquid. These observations demonstrated that PMO@ILCu<sub>2</sub>(OH)<sub>3</sub>Cl<sub>2</sub>(1.0) is thermally stable below 200 °C.

After the characterization of PMO@ILCu<sub>2</sub>(OH)<sub>3</sub>Cl<sub>2</sub>(x), we intended to examine the catalytic activity for the cycloaddition of propylene oxide with CO<sub>2</sub> to produce propylene carbonate, and the results are described in Table 1. The effect of benzotriazolium-based ionic liquid loading levels on PMO

**Fig. 7** Thermogravimetric analysis of PMO@ILCu<sub>2</sub>(OH)<sub>3</sub>Cl<sub>2</sub>(1.0)



was investigated (Table 1, entries 1–5), it was found that PMO@ILCu<sub>2</sub>(OH)<sub>3</sub>Cl<sub>2</sub>(1.0) possessed the highest catalytic activities of 97% yield with excellent selectivity 99.3% (Table 1, entry 4). The comparison was then carried out using bulk ionic liquid ILCu<sub>2</sub>(OH)<sub>3</sub>Cl<sub>2</sub>, ILCl, and PMO as catalysts (Table 1, entries 6–8) and they resulted in bad catalytic activity. As expected, no product was detected when the reaction was performed without a catalyst (Table 1, entry 9). The excellent activity observed for PMO@ILCu<sub>2</sub>(OH)<sub>3</sub>Cl<sub>2</sub>(1.0) confirms the most important copper oxychloride anion and PMO support for obtaining high catalytic activity for the synthesis of propylene carbonate under moderate reaction conditions. From the above studies, PMO@ILCu<sub>2</sub>(OH)<sub>3</sub>Cl<sub>2</sub>(1.0) could serve as the proper catalyst for the solvent-free cycloaddition. These results also revealed that the as-synthesized immobilized catalyst PMO@ILCu<sub>2</sub>(OH)<sub>3</sub>Cl<sub>2</sub>(1.0) contributes

to the enhancement of catalytic activity and selectivity, which was most likely due to the synergistic effect from hydroxyl active sites and strong nucleophilic anions with the appropriate cations that accelerates the CO<sub>2</sub> cycloaddition. The effect of catalyst amount on the cycloaddition reaction were studied. The conversion increased when the catalyst amount increased from 0.05 g to 0.2 g (Table 1, entries 3, 10–12), and best result was obtained with 0.2 g catalyst. However, it has been observed that further increase in the catalyst amount did not give more product (Table 1, entry 13). Therefore, 0.2 g catalyst of PMO@ILCu<sub>2</sub>(OH)<sub>3</sub>Cl<sub>2</sub>(1.0) was employed for further investigation.

The effects of reaction temperature on the cycloaddition were studied and results were displayed in Fig. 8a. With the increase in reaction temperature, the conversion of propylene oxide and the yield of propylene carbonate was significantly

**Table 1** Screening of catalysts for the synthesis of propylene carbonate

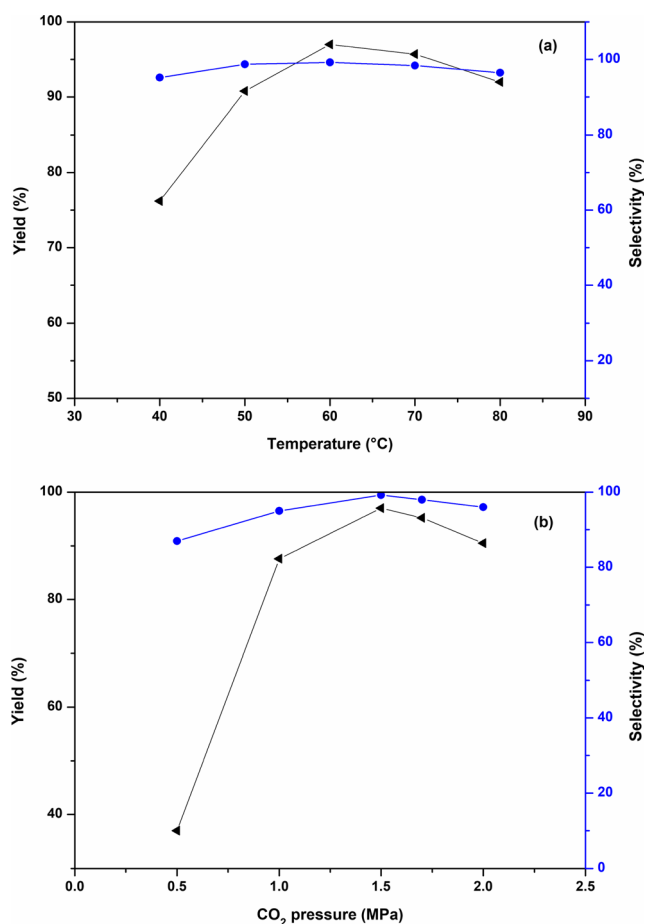
Entry	Catalyst	Catalyst (g)	Time (h)	Yield (%) <sup>a</sup>	Selectivity (%) <sup>b</sup>
1	PMO@ILCu <sub>2</sub> (OH) <sub>3</sub> Cl <sub>2</sub> (0.4)	0.2	5	79.5	98.6
2	PMO@ILCu <sub>2</sub> (OH) <sub>3</sub> Cl <sub>2</sub> (0.6)	0.2	3	88.4	98.4
3	PMO@ILCu <sub>2</sub> (OH) <sub>3</sub> Cl <sub>2</sub> (0.8)	0.2	2.5	93	99.1
4	PMO@ILCu <sub>2</sub> (OH) <sub>3</sub> Cl <sub>2</sub> (1.0)	0.2	2.5	97	99.3
5	PMO@ILCu <sub>2</sub> (OH) <sub>3</sub> Cl <sub>2</sub> (1.2)	0.2	2.5	96.7	99
6	ILCu <sub>2</sub> (OH) <sub>3</sub> Cl <sub>2</sub>	0.2 <sup>c</sup>	7	85	93.7
7	ILCl	0.2 <sup>c</sup>	12	43	89.4
8	PMO	0.2 <sup>c</sup>	12	18	86.5
9	–	–	24	0	0
10	PMO@ILCu <sub>2</sub> (OH) <sub>3</sub> Cl <sub>2</sub> (1.0)	0.05	4	57	99
11	PMO@ILCu <sub>2</sub> (OH) <sub>3</sub> Cl <sub>2</sub> (1.0)	0.1	4	81.7	99.3
12	PMO@ILCu <sub>2</sub> (OH) <sub>3</sub> Cl <sub>2</sub> (1.0)	0.15	2.5	93	99.2
13	PMO@ILCu <sub>2</sub> (OH) <sub>3</sub> Cl <sub>2</sub> (1.0)	0.25	2.5	96.5	99.2

Reaction conditions: propylene oxide (0.1 mmol), CO<sub>2</sub> pressure (1.5 MPa), catalyst, 60 °C.

<sup>a</sup> Isolated yields of pure products

<sup>b</sup> Determined by GC analysis

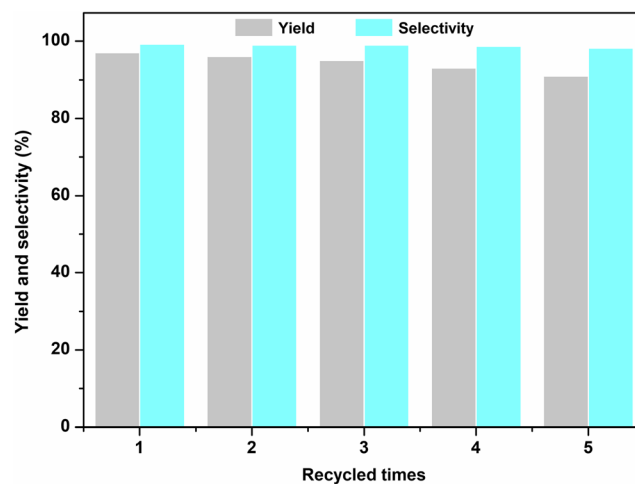
<sup>c</sup> Reaction temperature at 100 °C



**Fig. 8** (a) Effects of reaction temperature: propylene oxide (0.1 mmol), CO<sub>2</sub> pressure (1.5 MPa), PMO@ILCu<sub>2</sub>(OH)<sub>3</sub>Cl<sub>2</sub>(1.0) 0.2 g, 2.5 h; (b) Effects of initial pressure: propylene oxide (0.1 mmol), PMO@ILCu<sub>2</sub>(OH)<sub>3</sub>Cl<sub>2</sub>(1.0) 0.2 g, 60 °C, 2.5 h

increased, followed by a slight increase in the of propylene carbonate. However, the yield and selectivity of propylene carbonate exhibited a slight decrease after the temperature goes 60 °C. This may be due to the side reactions of isomerization and ring opening of propylene oxide occurred at overly high temperatures (determined by GC analysis). Thus, 60 °C was adopted as the appropriate reaction temperature. In addition, the effects of initial pressure on the catalytic was also investigated (Fig. 8b). It can be observed that the yield and selectivity of propylene carbonate were obviously facilitated when the increase CO<sub>2</sub> pressure from 0.5 MPa to 1.5 MPa, then displayed a visible decrease when CO<sub>2</sub> pressure was above 1.5 MPa. It was because higher CO<sub>2</sub> pressures caused the increased concentration of the substrates in the low-pressure region, thus resulting in high yields and selectivities. Too high CO<sub>2</sub> pressure may retard the interaction of the substrates and the catalyst, and reduced the propylene oxide concentration to give low yields and selectivities [13–16]. Hence, 1.5 MPa of carbon dioxide was the optimum pressure.

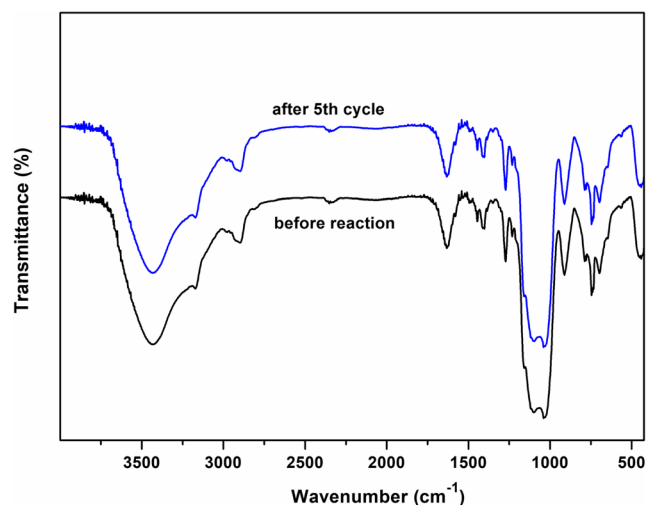
To test the reusability of the catalyst, the catalyst was easily recovered from the reaction mixture by filtration



**Fig. 9** Recyclability chart of PMO@ILCu<sub>2</sub>(OH)<sub>3</sub>Cl<sub>2</sub>(1.0)

and then reused directly for a subsequent similar reaction. We have examined the reusability of this heterogeneous catalyst for the cycloaddition of propylene oxide with CO<sub>2</sub> to produce propylene carbonate under the optimized reaction conditions (Fig. 9). It was observed that the catalyst could be recycled and reused for at least five consecutive runs without significant losses in its catalytic activity. The recovered catalyst after five runs was characterized by FT-IR, which showed similar spectra with fresh catalyst, indicating the stability of the catalyst (Fig. 10). In addition, SEM image of the recovered catalyst after five runs showed similar morphology to that of the original one (Fig. 4g). The above results provide further evidence for the high stability of the catalyst PMO@ILCu<sub>2</sub>(OH)<sub>3</sub>Cl<sub>2</sub>(1.0).


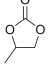
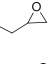
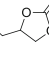
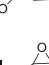
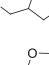
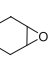
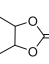
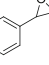
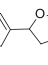
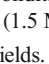
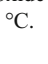
The catalytic performance of PMO@ILCu<sub>2</sub>(OH)<sub>3</sub>Cl<sub>2</sub>(1.0) has also been studied using other epoxides for the synthesis of corresponding cyclic carbonates. As can be seen in Table 2, the cycloaddition proceeded smoothly to give the



**Fig. 10** FT-IR spectra of PMO@ILCu<sub>2</sub>(OH)<sub>3</sub>Cl<sub>2</sub>(1.0) before reaction and after 5th cycle of the reaction



**Table 2** Cycloaddition of CO<sub>2</sub> to different epoxides over PMO@ILCu<sub>2</sub>(OH)<sub>3</sub>Cl<sub>2</sub>(1.0).

Entry	Epoxide	Product	Time (h)	Yield (%) <sup>a</sup>	Selectivity (%) <sup>b</sup>
1			2.5	97	99.3
2			2.5	95	99.5
3			2	98	99.4
4			2	93	99.2
5			5	88	99
6			4	90	99.1

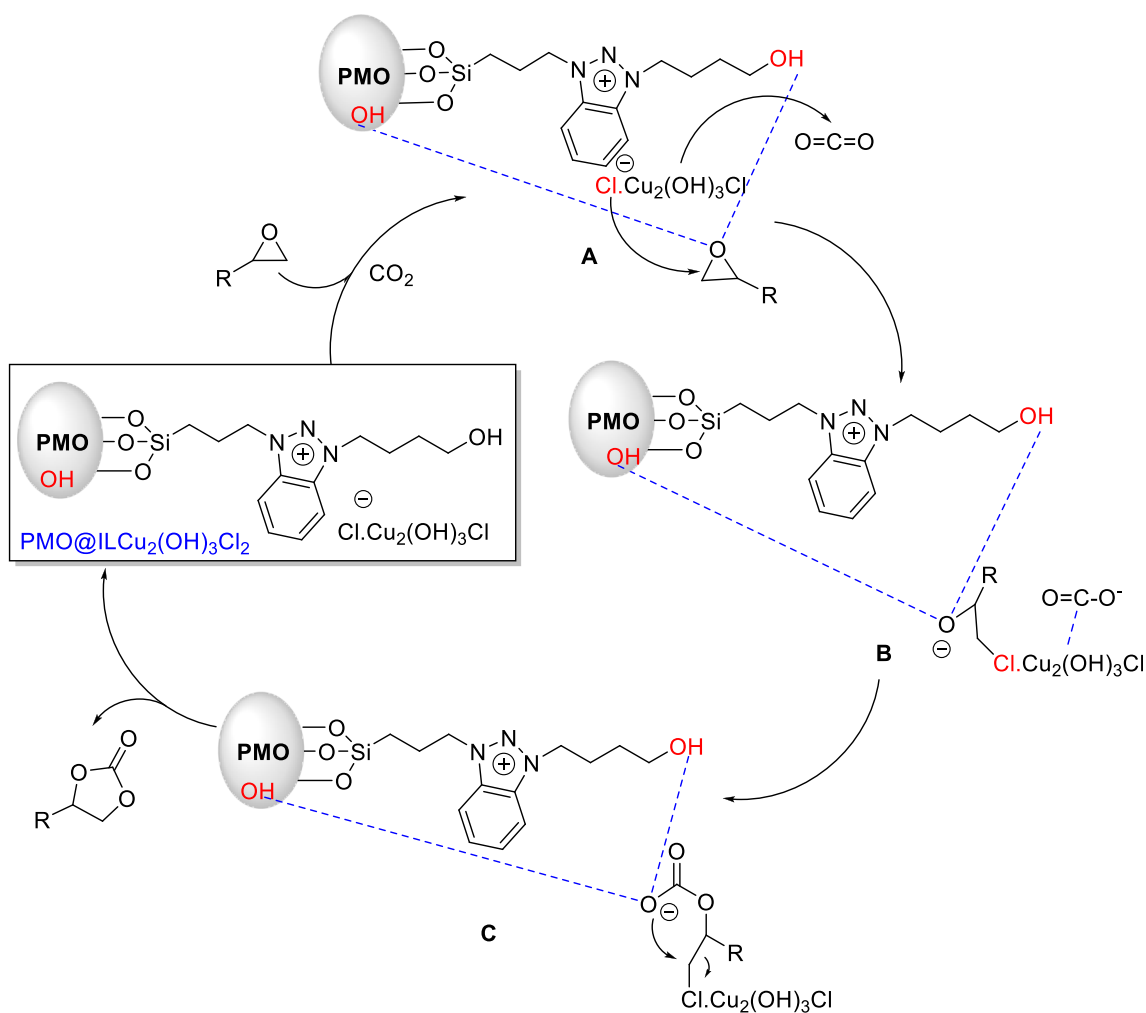
Reaction conditions: epoxide (0.1 mol), PMO@ILCu<sub>2</sub>(OH)<sub>3</sub>Cl<sub>2</sub>(1.0) 0.2 g, CO<sub>2</sub> (1.5 MPa), 60 °C.

<sup>a</sup> Isolated yields.

<sup>b</sup> Determined by GC analysis.

corresponding cyclic carbonates from the terminal epoxides within 5 h, which exhibited high yields (89% ~ 98%) and extremely excellent selectivities (99% ~ 99.5%). Pleasingly, epoxides containing electron withdrawing and electron donating groups were converted to the desired products and showed the good functional group tolerance. While the reaction of styrene oxide and cyclohexene oxide showed lower activity, and longer times needed to obtain good yields (Table 2, entries 5 and 6), probably due to the low reactivity of the β-carbon atom and the high steric hindrance of cyclohexene group.

Based on the above and other reported data in the literature [14–21], a possible mechanism is predicated as shown in Scheme 3. In the proposed catalytic cycle, epoxide could be activated through the coordination of hydroxyl group sites of PMO@ILCu<sub>2</sub>(OH)<sub>3</sub>Cl<sub>2</sub>(1.0) and the O atom of epoxide, resulting in the polarization of C–O bond, so as to form the intermediate **A**, together with the adsorption and activation of CO<sub>2</sub> by the alkaline anion of copper oxychloride to form carbonate species. Then, intermediate **B** is formed via an



**Scheme 3** Proposed reaction mechanism for the synthesis of cyclic carbonates

**Table 3** Comparison of as-prepared catalyst with various previously reported catalyst for cycloaddition of CO<sub>2</sub> to epoxides

Entry	Catalyst	Conditions	Time (h)	Yield/ Selectivity (%)	References
1	[La{N(SiHMe <sub>2</sub> ) <sub>2</sub> } <sub>2</sub> {κ <sup>3</sup> -bpzcp}]/TBAB	propylene oxide, CO <sub>2</sub> (1 MPa), 70 °C	16	95/95	[10]
2	DBU/NIS	cyclohexene oxide, CO <sub>2</sub> (0.1 MPa), 60 °C	12	37/–	[13]
3	lignin/KI	styrene oxide, CO <sub>2</sub> (2 MPa), 140 °C	12	87/–	[15]
4	B <sub>2</sub> O <sub>3</sub> / <i>n</i> -Bu <sub>4</sub> NBr	propylene oxide, CO <sub>2</sub> (2 MPa), 100 °C	2	90/99	[16]
5	amino-MIL-101(Al)@Fe <sub>3</sub> O <sub>4</sub> /SiO <sub>2</sub> /DMF	styrene oxide, CO <sub>2</sub> (0.1 MPa), 100 °C	16	80/100	[19]
6	NH <sub>3</sub> I-Zn/SBA-15 (0.12)	styrene oxide, CO <sub>2</sub> (0.1 MPa), 130 °C	12	71/99	[20]
7	WP-KI	propylene oxide, CO <sub>2</sub> (1.5 MPa), 120 °C	3	94/–	[21]
8	Ti(HPO <sub>4</sub> ) <sub>2</sub> ·H <sub>2</sub> O/ <i>n</i> -Bu <sub>4</sub> NBr	propylene oxide, CO <sub>2</sub> (1 MPa), R.T.	6	90/–	[25]
9	[P <sub>4</sub> 4 4 4][bzim]	cyclohexene oxide, CO <sub>2</sub> (1 MPa), 100 °C	3	71.2/99	[33]
10	PMO@ILCu <sub>2</sub> (OH) <sub>3</sub> Cl <sub>2</sub> (1.0)	propylene oxide, CO <sub>2</sub> (1.5 MPa), 60 °C	2.5	97/99.3	This work

nucleophilic attack on the less sterically hindered carbon atom of epoxide. After that, followed by the nucleophilic interaction of **B** and CO<sub>2</sub>, resulted in the formation of intermediate **C**. Subsequently, the intramolecular substitution of anion gave the final desired product and releases the catalyst for the next catalytic cycle. The presence of the alkaline anion of copper oxychloride probably have a synergetic effect on effective activation of CO<sub>2</sub> and presence of hydroxyl groups can significantly activate the epoxides, which provide sufficient catalytic sites and promote the catalytic cycloaddition.

To understand the advantage of the catalytic system, we compared the as-prepared catalyst with previously reported catalysts. As shown in Table 3, PMO@ILCu<sub>2</sub>(OH)<sub>3</sub>Cl<sub>2</sub>(1.0) catalyst presented superior features of excellent catalytic activities. These results demonstrated that the catalytic performance of PMO@ILCu<sub>2</sub>(OH)<sub>3</sub>Cl<sub>2</sub>(1.0) for the cycloaddition of CO<sub>2</sub> with epoxides to produce cyclic carbonates can be considered as quite promising, indicating that PMO@ILCu<sub>2</sub>(OH)<sub>3</sub>Cl<sub>2</sub>(1.0) is an *appropriate catalyst* for the cycloaddition of CO<sub>2</sub> to epoxides.

## 4 Conclusion

In conclusion, a novel type of copper oxychloride anionic benzotriazolium ionic liquid-modified periodic mesoporous organosilicas nanoparticles were synthesized, characterized and used as practical heterogeneous nanocatalysts for the synthesis of cyclic carbonates by the cycloaddition of CO<sub>2</sub> with epoxides. The synergistic effects between the hydroxyl groups sites on PMO framework and the active sites (hydroxyl groups/ copper oxychloride anion) of IL contributes to improving the catalytic sites of the catalyst. Among the different *loading* levels benzotriazolium-based ILs, PMO@ILCu<sub>2</sub>(OH)<sub>3</sub>Cl<sub>2</sub>(1.0) exhibited the most highly improved catalytic *activity* for the reaction with high yields and

selectivities *under solvent-* and cocatalyst-free conditions. Also, the catalyst PMO@ILCu<sub>2</sub>(OH)<sub>3</sub>Cl<sub>2</sub>(1.0) displayed high thermal stability and could be easily recovered and recycled for five runs. Notably, considering the homogeneous catalytic cycloaddition/heterogeneous separation of this nanocatalyst, an efficient and environmentally benign strategy has been developed for the chemical fixation of CO<sub>2</sub> with epoxides.

**Acknowledgments** The authors thank the Science and Technology Program of Jiangxi Provincial Education Bureau (No. GJJ180575) and Natural Science Foundation of Jiangxi Province of China (No. 20202BABL203023) for the support on this research.

## Compliance with Ethical Standards

**Conflict of interest** There is no conflict of interest for each contributing author.

## References

1. Tappe NA, Reich RM, D'Elia V, Kühn FE (2018) Dalton Trans 47: 13281–13313
2. Dalpozzo R, Ca ND, Gabriele B, Mancuso R (2019) Recent Advances in the Chemical Fixation of Carbon Dioxide: A Green Route to Carbonylated Heterocycle Synthesis. Catalysts 9:511
3. Mousavian S, Faravar P, Zarei Z, Azimikia R, Monjezi MG, Kianfar E (2020) Modeling and simulation absorption of CO<sub>2</sub> using hollow fiber membranes (HFM) with mono-ethanol amine with computational fluid dynamics. J Environ Chem Eng 8(4): 103946
4. Kianfar E, Pirouzfard V, Sakhaeinia H (2017) An experimental study on absorption/stripping CO<sub>2</sub> using mono-ethanol amine hollow fiber membrane contactor. J Taiwan Inst Chem Eng 80:954–962
5. Kianfar E, Salimi M, Kianfar F, Kianfar M, Razavikia SAH (2019) CO<sub>2</sub>/N<sub>2</sub> Separation Using Polyvinyl Chloride Iso-Phthalic Acid/Aluminium Nitrate Nanocomposite Membrane. Macromol Res 27(1):83–89
6. Salimi M, Pirouzfard V, Kianfar E (2017) Enhanced gas transport properties in silica nanoparticle filler-polystyrene nanocomposite membranes. Colloid Polym Sci 295(1):215–226

7. Kamphuis AJ, Picchioni F, Pescarmona PP (2019) CO<sub>2</sub>-fixation into cyclic and polymeric carbonates: principles and applications. *Green Chem* 21:406–448
8. Büttner H, Longwitz L, Steinbauer J, Wulf C, Werner T (2017) *Top Curr Chem* 375:50
9. Martín C, Fiorani G, Kleij AW (2015) Recent Advances in the Catalytic Preparation of Cyclic Organic Carbonates. *ACS Catal* 5: 1353–1370
10. Martinez J, Fernandez-Baeza J, Sanchez-Barba LF, Castro-Osma JA, Lara-Sanchez A, Otero A (2017) An Efficient and Versatile Lanthanum Heteroscorpionate Catalyst for Carbon Dioxide Fixation into Cyclic Carbonates. *ChemSusChem* 10:2886–2890
11. Meléndez DO, Lara-Sánchez A, Martínez J, Wu X, Otero A, Castro-Osma JA, North M, Rojas RS (2018). *ChemCatChem* 10: 2271–2277
12. Ahmadi F, Tangestaninejad S, Moghadam M, Mirkhani V, Mohammadpoor-Baltork I, Khosropour AR (2011) Highly efficient chemical fixation of carbon dioxide catalyzed by high-valent tetraphenylporphyrinatotin(IV) triflate. *Inorg Chem Commun* 14:1489–1493
13. Ma R, He LN, Liu XF, Liu X, Wang MY (2017) *J CO<sub>2</sub> Util* 19:28–32
14. Sopena S, Martin E, Escudero-Adán EC, Kleij AW (2017) Pushing the Limits with Squaramide-Based Organocatalysts in Cyclic Carbonate Synthesis. *ACS Catal* 7:3532–3539
15. Wu Z, Xie H, Yu X, Liu E (2013) Lignin-Based Green Catalyst for the Chemical Fixation of Carbon Dioxide with Epoxides To Form Cyclic Carbonates under Solvent-Free Conditions. *ChemCatChem* 5:1328–1333
16. Zhao LY, Chen JY, Li WC, Lu AH (2019) *J CO<sub>2</sub> Util* 29:172–178
17. Liang J, Huang YB, Cao R (2019). *Coordin Chem Rev* 378:32–65
18. Zhou Z, Yang L, Wang Y, He C, Duan C (2018) Recent Advance on Chemical Fixation of Carbon Dioxide by Metal-organic Frameworks as Heterogeneous Catalysts. *Curr Org Chem* 22:1809–1824
19. Nourian M, Zadehahmadi F, Kardanpour R, Tangestaninejad S, Moghadam M, Mirkhani V, Mohammadpoor-Baltork I, Bahadori M (2017) Chemical fixation of carbon dioxide catalyzed by magnetically recoverable NH<sub>2</sub>-MIL-101(Al) as an elegant nanoreactor. *Catal Commun* 94:42–46
20. Liu M, Liu B, Liang L, Wang F, Shi L, Sun J (2016) Design of bifunctional NH<sub>3</sub>I-Zn/SBA-15 single-component heterogeneous catalyst for chemical fixation of carbon dioxide to cyclic carbonates. *J Mol Catal A Chem* 418-419:78–85
21. Chang H, Li Q, Cui X, Wang H, Bu Z, Qiao C, Lin T (2018) *J CO<sub>2</sub> Util* 24:174–179
22. Yu SS, Liu XH, Ma JG, Niu Z, Cheng P (2016) *J CO<sub>2</sub> Util* 14:122–125
23. Prajapati PK, Kumar A, Jain SL (2018) First Photocatalytic Synthesis of Cyclic Carbonates from CO<sub>2</sub> and Epoxides Using CoPc/TiO<sub>2</sub> Hybrid under Mild Conditions. *ACS Sustain Chem Eng* 6:7799–7809
24. Chen JH, Deng CH, Fang S, Ma JG, Cheng P (2018). *Green Chem* 20:989–996
25. Chowdhury AH, Chowdhury IH, Islam SM (2019) Titanium Phosphate with Flower-like Morphology As an Effective Reusable Catalyst for Chemical Fixation of CO<sub>2</sub> at Mild Reaction Conditions. *Ind Eng Chem Res* 58:11779–11786
26. Milani JLS, Meireles AM, Cabral BN, Bezerra WA, Martins FT, Martins DCS, Chagas RP (2019) *J CO<sub>2</sub> Util* 30:100–106
27. Zhang SJ, Lu XM (2006) *Ionic liquids: from fundamental research to industrial applications*. Science Press, Beijing
28. Costa JAS, Vedovello P, Paranhos CM (2020) Use of Ionic Liquid as Template for Hydrothermal Synthesis of the MCM-41 Mesoporous Material. *Silicon* 12:289–294
29. Asim AM, Uroos M, Naz S, Sultan M, Griffin G, Muhammad N, Khan AS (2019) Acidic ionic liquids: Promising and cost-effective solvents for processing of lignocellulosic biomass. *J Mol Liq* 287: 110943
30. Cheng C, Zhang C, Jiang J, Wang J, Bai J, Yuan W, Wang L (2019) Recycling of Polysilicon Byproduct SiCl<sub>4</sub> Dissolved in Ionic Liquids. *Silicon* 11:909–917
31. Prodius D, Mudring AV (2018) Rare earth metal-containing ionic liquids. *Coordin Chem Rev* 363:1–16
32. Dengler JE, Doroodian A, Rieger B (2011) Protic metal-containing ionic liquids as catalysts: Cooperative effects between anion and cation. *J Organomet Chem* 696:3831–3835
33. Goodrich P, Gunaratne HQN, Jacquemin J, Jin L, Lei Y, Seddon KR (2017) Sustainable Cyclic Carbonate Production, Utilizing Carbon Dioxide and Azolate Ionic Liquids. *ACS Sustain Chem Eng* 5:5635–5641
34. Honores J, Quezada D, Chacón G, Martínez-Ferraté O, Isaacs M (2019) Synthesis of Cyclic Carbonates from CO<sub>2</sub> and Epoxide Catalyzed by Co, Ni and Cu Complexes in Ionic Liquids. *Catal Lett* 149:1825–1832
35. He Q, O'Brien JW, Kitselman KA, Tompkins LE, GCT C, Kerton FM (2014) Synthesis of cyclic carbonates from CO<sub>2</sub> and epoxides using ionic liquids and related catalysts including choline chloride-metal halide mixtures. *Catal Sci Technol* 4:1513–1528
36. Vieira MO, Monteiro WF, Neto BS, Ligabue R, Chaban VV, Einloft S (2018) Surface Active Ionic Liquids as Catalyst for CO<sub>2</sub> Conversion to Propylene Carbonate. *Catal Lett* 148:108–118
37. Song YY, Jin QR, Zhang SL, Jing HW, Zhu QQ (2011) Chiral metal-containing ionic liquid: Synthesis and applications in the enantioselective cycloaddition of carbon dioxide to epoxides. *Sci China Chem* 54:1044–1050
38. Kianfar E, Salimi M, Pirouzfard V, Koohestani B (2018). *Int J Chem React Eng* 16(7):20170229
39. Kianfar E, Salimi M, Hajimirzaee S, Koohestani B (2019). *Int J Chem React Eng* 17(2):20180127
40. Kianfar E (2019) Nanozeolites: synthesized, properties, applications. *J Sol-Gel Sci Techn* 91(2):415–429
41. Kianfar E (2018) Synthesis and Characterization of AlPO<sub>4</sub>/ZSM-5 Catalyst for Methanol Conversion to Dimethyl Ether. *Russ J Appl Chem* 91(10):1711–1720
42. Kianfar E (2019) Ethylene to Propylene over Zeolite ZSM-5: Improved Catalyst Performance by Treatment with CuO. *Russ J Appl Chem* 92(7):933–939
43. Kianfar E (2019) Ethylene to Propylene Conversion over Ni-W/ZSM-5 Catalyst. *Russ J Appl Chem* 92(8):1094–1101
44. Kianfar E (2019) Comparison and assessment of zeolite catalysts performance dimethyl ether and light olefins production through methanol: a review. *Rev Inorg Chem* 39(3):157–177
45. Kianfar E, Salimi M, Pirouzfard V, Koohestani B (2018) Synthesis of modified catalyst and stabilization of CuO/NH<sub>4</sub>-ZSM-5 for conversion of methanol to gasoline. *Int J Appl Ceram Technol* 15(3): 734–741
46. Kianfar E, Azimikia R, Faghieh SM (2020) Simple and Strong Dative Attachment of  $\alpha$ -Diimine Nickel (II) Catalysts on Supports for Ethylene Polymerization with Controlled Morphology. *Catal Lett* 150:2322–2330
47. Kianfar E, Hajimirzaee S, Musavian S, Mehr AS (2020) Zeolite-based catalysts for methanol to gasoline process: A review. *Microchem J* 156:104822
48. Fehrmann R, Riisager A, Haumann M (2014) *Supported ionic liquids: fundamentals and applications*. Weinheim, Wiley-VCH Verlag
49. Bahadori M, Tangestaninejad S, Bertmer M, Moghadam M, Mirkhani V, Mohammadpoor-Baltork I, Kardanpour R, Zadehahmadi F (2019) Task-Specific Ionic Liquid Functionalized-MIL-101(Cr) as a Heterogeneous and Efficient Catalyst for the Cycloaddition of CO<sub>2</sub> with Epoxides Under Solvent Free Conditions. *ACS Sustain Chem Eng* 7:3962–3973

50. Muniandy L, Adam F, Rahman NRA, Ng EP (2019) Highly selective synthesis of cyclic carbonates via solvent free cycloaddition of CO<sub>2</sub> and epoxides using ionic liquid grafted on rice husk derived MCM-41. *Inorg Chem Commun* 104:1–7
51. Boroujeni KP, Ghasemi P, Rafienia Z (2014) Synthesis of biscoumarin derivatives using poly(4-vinylpyridine)-supported dual acidic ionic liquid as a heterogeneous catalyst. *Monatsh Chem* 145:1023–1026
52. Zand HRE, Ghafuri H, Rashidizadeh A, Khoushab Z (2019) Study on Oxidative Condensation of Toluene and Hydrazine/Aniline Catalyzed by Copper Complex Immobilized on Functionalized Graphene Oxide. *Ind Eng Chem Res* 58:5379–5387
53. Xia X, Hu G, Li W, Li S (2019) Understanding Reduced CO<sub>2</sub> Uptake of Ionic Liquid/Metal–Organic Framework (IL/MOF) Composites. *ACS Appl Nano Mater* 2:6022–6029
54. Andrade LS, Castanheira B, Brochsztain S (2020) Periodic mesoporous organosilicas containing naphthalenediimides within the pore walls for asphaltene adsorption. *Micropor Mesopor Mater* 294:109909
55. Manchanda AS (2015) Large-pore mesoporous organosilicas and related polymer nanocomposites. *CUNY Academic Works*
56. Kao HM, Chung CH, Saikia D, Liao SH, Chao PY, Chen YH, Wu KCW (2012) Highly Carboxylic-Acid-Functionalized Ethane-Bridged Periodic Mesoporous Organosilicas: Synthesis, Characterization, and Adsorption Properties. *Chem Asian J* 7: 2111–2117
57. Birault A, Molina E, Trens P, Cot D, Toquer G, Marcotte N, Carcel C, Bartlett JR, Gérardin C, Man MWC (2019) Periodic Mesoporous Organosilicas from Polyion Complex Micelles - Effect of Organic Bridge on Nanostructure. *Eur J Inorg Chem* 2019:3157–3164
58. Shylesh S, Srilakshmi C, Singh AP, Anderson BG (2007) One step synthesis of chromium-containing periodic mesoporous organosilicas and their catalytic activity in the oxidation of cyclohexane. *Micropor Mesopor Mater* 99:334–344
59. Lin F, Meng X, Kukueva E, Altantzis T, Mertens M, Bals S, Cool P, Doorslaer SV (2015) Direct-synthesis method towards copper-containing periodic mesoporous organosilicas: detailed investigation of the copper distribution in the material. *Dalton Trans* 44: 9970–9979
60. Deka JR, Kao HM, Huang SY, Chang WC, Ting CC, Rath PC, Chen CS (2014) Ethane-Bridged Periodic Mesoporous Organosilicas Functionalized with High Loadings of Carboxylic Acid Groups: Synthesis, Bifunctionalization, and Fabrication of Metal Nanoparticles. *Chem Eur J* 20:894–903
61. Wang X, Thiel I, Fedorov A, Copéret C, Mougél V, Fontecave M (2017) Site-isolated manganese carbonyl on bipyridine-functionalities of periodic mesoporous organosilicas: efficient CO<sub>2</sub> photoreduction and detection of key reaction intermediates. *Chem Sci* 8:8204–8213
62. Karimi B, Elhamifar D, Yari O, Khorasani M, Vali H, Clark JH, Hunt AJ (2012) Synthesis and Characterization of Alkyl-Imidazolium-Based Periodic Mesoporous Organosilicas: A Versatile Host for the Immobilization of Perruthenate (RuO<sub>4</sub><sup>-</sup>) in the Aerobic Oxidation of Alcohols. *Chem Eur J* 18:13520–13530
63. Takeda H, Ohashi M, Goto Y, Ohsuna T, Tani T, Inagaki S (2016) A Versatile Solid Photosensitizer: Periodic Mesoporous Organosilicas with Ruthenium Tris(bipyridine) Complexes Embedded in the Pore Walls. *Adv Funct Mater* 26:5068–5077
64. Doustkhah E, Mohtasham H, Hasani M, Ide Y, Rostamnia S, Tsunogi N, Assadi MHN (2020) Merging periodic mesoporous organosilica (PMO) with mesoporous aluminosilica (Al/Si-PMO): A catalyst for green oxidation. *Mol Catal* 482:110676
65. Bakshi PS, Gusain R, Dhawaria M, Suman SK, Khatri OP (2016) Antimicrobial and lubrication properties of 1-acetyl-3-hexylbenzotriazolium benzoate/sorbate ionic liquids. *RSC Adv* 6: 46567–46572
66. Wang G, Huang B, Li Z, Wang Z, Qin X, Zhang X, Dai Y, Whangbo MH (2015) On Structural Features Necessary for Near-IR-Light Photocatalysts. *Chem Eur J* 21:13583–13587
67. Han MS, Lee BG, Ahn BS, Moon DJ, Hong SI (2003) Surface properties of CuCl<sub>2</sub>/AC catalysts with various Cu contents: XRD, SEM, TG/DSC and CO-TPD analyses. *Appl Surf Sci* 211:76–81
68. Kwak JH, Varga T, Peden CHF, Gao F, Hanson JC, Szanyi J (2014) Following the movement of Cu ions in a SSZ-13 zeolite during dehydration, reduction and adsorption: A combined in situ TP-XRD, XANES/DRIFTS study. *J Catal* 314:83–93

**Publisher's Note** Springer Nature remains neutral with regard to jurisdictional claims in published maps and institutional affiliations.